COMPUTATION OF THREE-DIMENSIONAL ELECTROMAGNETIC-FIELD DISTRIBUTIONS IN A HUMAN BODY USING THE WEAK FORM OF THE CGFFT METHOD

A. Peter M. Zwamborn*, Peter M. van den Berg*, Jaap Mooibroek and Fred T.C. Koenis*****

* Laboratory for Electromagnetic Research
Department of Electrical Engineering
Delft University of Technology
P.O. Box 5031, 2600 GA Delft
The Netherlands

** Department of Radiotherapy
University Hospital Utrecht
Heidelberglaan 100, 3584 CX Utrecht
The Netherlands

*** Department of Radiotherapy
Academic Medical Centre
University of Amsterdam
Meibergdreef 9, 1105 AZ Amsterdam
The Netherlands

Abstract

The problem of the computation of electromagnetic-field distributions in a strongly inhomogeneous human body is formulated in terms of an integral equation over the body. A weak form of the integral equation is discussed, in which the spatial derivatives occurring in this equation are integrated analytically. The resulting equation can then be solved very efficiently using the advantageous combination of a conjugate-gradient iterative method and a fast Fourier technique (CGFFT). Numerical calculations have been carried out for a strongly inhomogeneous, lossy radially layered sphere. A comparison with the Mie-series solution shows that the present weak form of the CGFFT method yields accurate results. The absorbed power density inside a CAT-scan generated model of the body of one of the authors is computed. It demonstrates that the present method can be considered as a comparatively simple and efficient tool for solving electromagnetic wave-field problems in strongly inhomogeneous bodies.

1. Introduction

During the past several years considerable effort has been put into the development of efficient techniques for computation of electromagnetic wave fields in a strongly inhomogeneous object. One of the extensively utilized methods is the domain-integral-equation technique. It takes into account that the irradiated object is present in free space and that it manifests itself through the presence of secondary sources of contrast currents. The first method for solving the electric-field integral equation over the domain of a dielectric object was developed by Richmond for the two-dimensional TM case [Richmond, 1965], and for the two-dimensional TE case [Richmond, 1966]. Here the method of moments has been used with pulse expansion functions and point matching. The use of pulse expansion functions in the TE-case leads to numerical errors [Massoudi et al., 1984, Hagmann, 1985]. The method of moments requires the inversion of a (large) matrix, limiting the application of this

method. This problem has been circumvented by using a conjugate-gradient iterative technique [Van den Berg, 1984]. Bojarski [1982] has introduced the k-space method, obtaining an iterative approach that reduces the storage and the computation time by using a fast Fourier transform algorithm for the computation of the spatial convolution that occurs in the integral equation. A comprehensive review of Bojarski's work, together with the appropriate references to his k-space frequency domain method, can be found in his 1982 k-space time-domain paper.

In the numerical solution of two-dimensional TE and three-dimensional scattering problems, the applicability of the conjugate-gradient FFT method using pulse expansion functions casts some serious doubts [Borup et al., 1987, Joachimowicz and Pichot, 1990]. The operator involved consists of a grad-div operator that acts on a vector potential. The vector potential is an integral of the product of a Green's function and the electric contrast-current density inside the object. The vector potential is a spatial convolution. In the spectral Fourier domain this convolution is algebraic: a simple product. Recently, the weak formulation of the conjugate-gradient FFT method has proved to be an efficient and accurate scheme for solving two-dimensional TE scattering by strongly inhomogeneous lossy dielectric objects [Zwamborn and Van den Berg, 1991a]. Therefore, in this present paper, we present a weak formulation of the domain-integral equation for the modeling of *full vectorial, three-dimensional*, electromagnetic wave-field problems. The domain-integral equation that is obtained in its strong form is weakened by testing it with appropriate testing functions. This weak form is the operator equation to be solved by a CGFFT method. The advantages of this procedure are, firstly, that the grad-div operator acting on the vector potential is integrated analytically over the domain of the dielectric object only and, secondly, that we have maintained the simple scalar form of the convolution structure of the vector potential (in fact three scalar convolutions). The integral equation is formulated in terms of the unknown electric-flux density rather than in terms of the electric-field strength. The continuity of the normal component of the electric-flux density yields a correct implementation of the boundary condition of the normal component of the electric field at the interfaces of (strong) discontinuity. In contrast to the weak formulation of the two-dimensional TE-case [Zwamborn and Van den Berg, 1991a], the three-dimensional formulation is presented for different mesh sizes in the three Cartesian coordinates.

We present some numerical results for three-dimensional problems. Numerical computations have been carried out for a strongly inhomogeneous, lossy radially layered sphere. These numerical results are compared with existing analytical solutions (Mie series) and it is directly observed that the weak form of the conjugate-gradient FFT method yields accurate results. Subsequently, the absorbed power density inside a realistic model of the body of one of the authors, the Jaap phantom, is computed. These two test cases demonstrate that the present weak formulation of the conjugate-gradient FFT method can be considered to be a comparatively simple and efficient tool for solving scattering problems pertaining to (strongly) inhomogeneous lossy dielectric objects.

2. The domain-integral equation

The vectorial position in the three-dimensional space is denoted by $\boldsymbol{x} = (x_1, x_2, x_3)$. The unit vectors in the x_1-, x_2- and x_3-directions are given by $\boldsymbol{i}_1, \boldsymbol{i}_2$ and $\boldsymbol{i}_3$. The time factor $\exp(-i\omega t)$ has been used for the field quantities in the frequency domain. We consider the problem of scattering by a lossy inhomogeneous dielectric object with complex permittivity

$$\varepsilon(\boldsymbol{x}) = \varepsilon_r(\boldsymbol{x})\varepsilon_0 + i\frac{\sigma(\boldsymbol{x})}{\omega}, \tag{1}$$

where ε_r denotes the relative permittivity of the object with respect to the lossless and homogeneous embedding with permittivity ε_0, and where σ denotes the electric conductivity of the object. The incident electric field is denoted as $\mathbf{E}^i = (E_1^i, E_2^i, E_3^i)$. In this paper, we formulate the scattering problem as a domain-integral equation for the unknown electric-flux density $\mathbf{D} = (D_1, D_2, D_3)$ over

the object domain $\mathbb{D}^S$ as

$$\mathbf{E}^i(\boldsymbol{x}) = \frac{\mathbf{D}(\boldsymbol{x})}{\varepsilon(\boldsymbol{x})} - (k_0^2 + \text{grad div})\mathbf{A}(\boldsymbol{x}), \quad \boldsymbol{x} \in \mathbb{D}^S. \tag{2}$$

where $k_0 = \omega(\varepsilon_0\mu_0)^{\frac{1}{2}}$ and the vector potential $\mathbf{A} = (A_1, A_2, A_3)$ is given by

$$\mathbf{A}(\boldsymbol{x}) = \frac{1}{\varepsilon_0}\int_{\boldsymbol{x}'\in\mathbb{D}^S} G(\boldsymbol{x}-\boldsymbol{x}')\chi(\boldsymbol{x}')\mathbf{D}(\boldsymbol{x}')d\boldsymbol{x}', \tag{3}$$

in which the normalized contrast function χ is defined as

$$\chi(\boldsymbol{x}) = \frac{\varepsilon(\boldsymbol{x}) - \varepsilon_0}{\varepsilon(\boldsymbol{x})}. \tag{4}$$

Further, the three-dimensional Green's function G is given by

$$G(\boldsymbol{x}) = \frac{\exp(ik_0|\boldsymbol{x}|)}{4\pi|\boldsymbol{x}|}, \quad \boldsymbol{x} \in \mathbb{R}^3. \tag{5}$$

Eqs. (2) - (5) are equations in a strong form. In the next section we shall present a weak form.

3. The weak form

We first introduce a discretization in the spatial domain $\boldsymbol{x} = (x_1, x_2, x_3)$. We use a uniform mesh with grid widths of Δx_1, Δx_2 and Δx_3 in the x_1, x_2 and x_3 directions, respectively. For our convenience the discrete values of $\boldsymbol{x}$ are given by

$$\boldsymbol{x}_{M,N,P} = \left\{(M-\frac{1}{2})\Delta x_1, (N-\frac{1}{2})\Delta x_2, (P-\frac{1}{2})\Delta x_3\right\}, \tag{6}$$

denoting the centerpoints of the volumetric subdomains. The boundary of the discretized object now consists of surfaces parallel to the x_1-, x_2- or x_3-axis. We assume that the discretized boundary $\partial\mathbb{D}^S$ of the object domain $\mathbb{D}^S$ lies completely in the embedding where $\chi = 0$. This is always possible, since we can extend the definition of the object domain $\mathbb{D}^S$ by extending it with a zero contrast function χ. In each volumetric subdomain with center $\boldsymbol{x}_{M,N,P}$ and dimension $\Delta x_1 \times \Delta x_2 \times \Delta x_3$, we assume the complex permittivity to be constant with values $\varepsilon_{M,N,P}$. Note that jumps in the (complex) permittivity function may occur at $x_1 = M\Delta x_1$, $x_2 = N\Delta x_2$ and $x_3 = P\Delta x_3$.

In order to cope with the grad-div operator in Eq. (2), we test the strong form of Eq. (2) by multiplying both the sides of the equality sign by a vectorial testing function $\boldsymbol{\psi}^{(p)}_{M,N,P}(\boldsymbol{x})$, $p = 1, 2, 3$, and integrate the result over the domain $\boldsymbol{x} \in \mathbb{D}^S$ upon using Gauss' theorem on each subdomain where $\partial_p\psi^{(p)}_{M,N,P}(\boldsymbol{x})$ div $\mathbf{A}(\boldsymbol{x})$ is continuously differentiable and by using the continuity of the normal component of this function through the interfaces between these subdomains. Subsequently, we expand the generalized electric-flux density, the electric-contrast vector potential and the incident electric field in a sequence of vectorial expansion functions $\boldsymbol{\psi}^{(q)}_{I,J,K}(\boldsymbol{x}) = \psi^{(q)}_{I,J,K}(\boldsymbol{x})\boldsymbol{i}_q$, $q = 1, 2, 3$ and obtain

$$D_q(\boldsymbol{x}) = \varepsilon_0 \sum_{I,J,K} d^{(q)}_{I,J,K}\psi^{(q)}_{I,J,K}(\boldsymbol{x}) \quad \text{for } \boldsymbol{x} \in \mathbb{D}^S, \tag{7}$$

$$A_q(\boldsymbol{x}) = \sum_{I,J,K} A^{(q)}_{I,J,K}\psi^{(q)}_{I,J,K}(\boldsymbol{x}) \quad \text{for } \boldsymbol{x} \in \mathbb{D}^S, \tag{8}$$

$$E^i_q(\boldsymbol{x}) = \sum_{I,J,K} E^{i,(q)}_{I,J,K}\psi^{(q)}_{I,J,K}(\boldsymbol{x}) \quad \text{for } \boldsymbol{x} \in \mathbb{D}^S. \tag{9}$$

In view of the partial derivatives acting on the testing and expansion functions, the volumetric rooftop functions [Catedra et al., 1989] are chosen as basis in the test and expansion functions.

Using these functions we obtain the following weak formulation of the domain-integral equation, see [Zwamborn, 1991b, Zwamborn and Van den Berg, 1992],

$$
\begin{aligned}
e^{i,(1)}_{M,N,P} &= \sum_{I=1}^{3}\left[b^{(1)}_I d^{(1)}_{M+I-2,N,P} + c^{(1)}_I A^{(1)}_{M+I-2,N,P}\right] + \sum_{I=1}^{2}\sum_{J=1}^{2} t^{(3)}_{I,J} A^{(2)}_{M+I-2,N+J-1,P} \\
&\quad + \sum_{I=1}^{2}\sum_{K=1}^{2} t^{(2)}_{I,K} A^{(3)}_{M+I-2,N,P+K-1}, \qquad (10)\\
e^{i,(2)}_{M,N,P} &= \sum_{I=1}^{2}\sum_{J=1}^{2} t^{(3)}_{J,I} A^{(1)}_{M+I-1,N+J-2,P} + \sum_{J=1}^{3}\left[b^{(2)}_J d^{(2)}_{M,N+J-2,P} + c^{(2)}_J A^{(2)}_{M,N+J-2,P}\right] \\
&\quad + \sum_{J=1}^{2}\sum_{K=1}^{2} t^{(1)}_{J,K} A^{(3)}_{M,N+J-2,P+K-1}, \qquad (11)\\
e^{i,(3)}_{M,N,P} &= \sum_{I=1}^{2}\sum_{K=1}^{2} t^{(2)}_{K,I} A^{(1)}_{M+I-1,N,P+K-2} + \sum_{J=1}^{2}\sum_{K=1}^{2} t^{(1)}_{K,J} A^{(2)}_{M,N+J-1,P+K-2} \\
&\quad + \sum_{K=1}^{3}\left[b^{(3)}_K d^{(3)}_{M,N,P+K-2} + c^{(3)}_K A^{(3)}_{M,N,P+K-2}\right], \qquad (12)
\end{aligned}
$$

in which the coefficients of the vectors $\mathbf{b}^{(p)}$ and $\mathbf{c}^{(p)}$ are obtained as

$$
\mathbf{b}^{(1)} = \frac{\Delta x_1 \Delta x_2 \Delta x_3}{6}\begin{pmatrix} \dfrac{\varepsilon_0}{\varepsilon_{M-1,N,P}} \\ \dfrac{2\varepsilon_0}{\varepsilon_{M-1,N,P}} + \dfrac{2\varepsilon_0}{\varepsilon_{M,N,P}} \\ \dfrac{\varepsilon_0}{\varepsilon_{M,N,P}} \end{pmatrix}, \qquad (13)
$$

$$
\mathbf{b}^{(2)} = \frac{\Delta x_1 \Delta x_2 \Delta x_3}{6}\begin{pmatrix} \dfrac{\varepsilon_0}{\varepsilon_{M,N-1,P}} \\ \dfrac{2\varepsilon_0}{\varepsilon_{M,N-1,P}} + \dfrac{2\varepsilon_0}{\varepsilon_{M,N,P}} \\ \dfrac{\varepsilon_0}{\varepsilon_{M,N,P}} \end{pmatrix}, \qquad (14)
$$

$$
\mathbf{b}^{(3)} = \frac{\Delta x_1 \Delta x_2 \Delta x_3}{6}\begin{pmatrix} \dfrac{\varepsilon_0}{\varepsilon_{M,N,P-1}} \\ \dfrac{2\varepsilon_0}{\varepsilon_{M,N,P-1}} + \dfrac{2\varepsilon_0}{\varepsilon_{M,N,P}} \\ \dfrac{\varepsilon_0}{\varepsilon_{M,N,P}} \end{pmatrix}, \qquad (15)
$$

$$\mathbf{c}^{(p)} = \Delta x_1 \Delta x_2 \Delta x_3 \left[-\frac{k_0^2}{6} \begin{pmatrix} 1 \\ 4 \\ 1 \end{pmatrix} + (\Delta x_p)^{-2} \begin{pmatrix} -1 \\ 2 \\ -1 \end{pmatrix} \right], \tag{16}$$

while the coefficients of the matrix $\mathbf{t}^{(p)}$ follow from

$$\mathbf{t}^{(p)} = \Delta x_p \begin{pmatrix} -1 & 1 \\ 1 & -1 \end{pmatrix}. \tag{17}$$

The values of $e^{i,(p)}_{M,N,P}$ follow from $E^{i,(p)}_{M,N,P}$ as

$$e^{i,(1)}_{M,N,P} = \frac{\Delta x_1 \Delta x_2 \Delta x_3}{6} \left[E^{i,(1)}_{M+1,N,P} + 4E^{i,(1)}_{M,N,P} + E^{i,(1)}_{M-1,N,P} \right], \tag{18}$$

$$e^{i,(2)}_{M,N,P} = \frac{\Delta x_1 \Delta x_2 \Delta x_3}{6} \left[E^{i,(2)}_{M,N+1,P} + 4E^{i,(2)}_{M,N,P} + E^{i,(2)}_{M,N-1,P} \right], \tag{19}$$

$$e^{i,(3)}_{M,N,P} = \frac{\Delta x_1 \Delta x_2 \Delta x_3}{6} \left[E^{i,(3)}_{M,N,P+1} + 4E^{i,(3)}_{M,N,P} + E^{i,(3)}_{M,N,P-1} \right]. \tag{20}$$

With our particular choice of expansion functions, the quantities $d^{(p)}_{M,N,P}$, $A^{(p)}_{M,N,P}$ and $e^{i,(p)}_{M,N,P}$ follow from

$$d^{(p)}_{M,N,P} = \frac{D_p(\boldsymbol{x}_{M,N,P} - \frac{1}{2}\Delta x_p \boldsymbol{i}_p)}{\varepsilon_0}, \quad p=1,2,3, \tag{21}$$

$$A^{(p)}_{M,N,P} = A_p(\boldsymbol{x}_{M,N,P} - \tfrac{1}{2}\Delta x_p \boldsymbol{i}_p), \quad p=1,2,3, \tag{22}$$

$$E^{i,(p)}_{M,N,P} = E^i_p(\boldsymbol{x}_{M,N,P} - \tfrac{1}{2}\Delta x_p \boldsymbol{i}_p), \quad p=1,2,3. \tag{23}$$

The electric-contrast vector potential A_m is related to the electric-flux density $\mathbf{D}$ via Eq. (3). Note that with this procedure we have enforced the equality sign of Eqs. (21) - (23) exactly in a single point. Again, this is a strong form and we will weaken this form by taking the spherical mean. The computation of the electric contrast-vector potential is discussed in [Zwamborn, 1991b, Zwamborn and Van den Berg, 1992] and we will only summarize the results.

Replacing the continuous convolution integral of Eq. (3) and using the convolution theorem of the discrete Fourier transform (DFT), the discrete convolution is evaluated numerically by

$$A^{(p)}_{M,N,P} = \Delta x_1 \Delta x_2 \Delta x_3 \mathrm{DFT}^{-1} \left\{ \mathrm{DFT}\left\{ G_{M',N',P'} \right\} \mathrm{DFT}\left\{ \chi^{(p)}_{M,N,P} d^{(p)}_{M,N,P} \right\} \right\}, \tag{24}$$

in which $p = 1, 2, 3$; the discrete values of the normalized contrast function follow from

$$\chi^{(1)}_{M,N,P} = \frac{\chi(\boldsymbol{x}_{M-1,N,P}) + \chi(\boldsymbol{x}_{M,N,P})}{2}, \tag{25}$$

$$\chi^{(2)}_{M,N,P} = \frac{\chi(\boldsymbol{x}_{M,N-1,P}) + \chi(\boldsymbol{x}_{M,N,P})}{2}, \tag{26}$$

$$\chi^{(3)}_{M,N,P} = \frac{\chi(\boldsymbol{x}_{M,N,P-1}) + \chi(\boldsymbol{x}_{M,N,P})}{2}. \tag{27}$$

The discrete values of the weakened Green's function are given by

$$G_{M,N,P} = [G](M\Delta x_1, N\Delta x_2, P\Delta x_3), \tag{28}$$

where

$$[G](\boldsymbol{x}) = \begin{cases} \dfrac{(1-\frac{1}{2}ik_0\Delta x)\exp(\frac{1}{2}ik_0\Delta x)-1}{\frac{1}{6}\pi k_0^2(\Delta x)^3} & \text{if } |\boldsymbol{x}|=0, \\ \dfrac{\exp(ik_0|\boldsymbol{x}|)\left[\dfrac{\sinh(\frac{1}{2}ik_0\Delta x)}{\frac{1}{2}ik_0\Delta x}-\cosh(\frac{1}{2}ik_0\Delta x)\right]}{\frac{1}{3}\pi(k_0\Delta x)^2|\boldsymbol{x}|} & \text{if } |\boldsymbol{x}|>\frac{1}{2}\Delta x. \end{cases} \tag{29}$$

Note that, for the limiting case $\Delta x \to 0$, the weak form of the Green's function $[G](\boldsymbol{x})$, $|\boldsymbol{x}| > \frac{1}{2}\Delta x$, tends to the strong form of the Green's function $G(\boldsymbol{x})$. The subscripts M', N' and P' of $G_{M',N',P'}$ in Eq. (24) are dictated by Eq. (6) and the spatial periodicity of the discrete Fourier transform.

Let us assume that the domain $\mathbb{D}^S$ of the object lies completely inside a block with $M_{\mathbb{D}^S}$ meshpoints in the x_1-direction, $N_{\mathbb{D}^S}$ meshpoints in the x_2-direction and $P_{\mathbb{D}^S}$ meshpoints in the x_3-direction. It is easily shown [Zwamborn, 1991b, Zwamborn and Van den Berg, 1992] that the numerical evaluation of Eq. (3) using a trapezoidal integration rule is equivalent with Eq. (24) inside the object domain $\mathbb{D}^S$ if the relevant DFT's are defined inside a block with M_{DFT} meshpoints in the x_1-direction, N_{DFT} meshpoints in the x_2-direction and P_{DFT} meshpoints in the x_3-direction, such that

$$M_{\mathrm{DFT}} \geq 2(M_{\mathbb{D}^S}+1), \quad N_{\mathrm{DFT}} \geq 2(N_{\mathbb{D}^S}+1), \quad P_{\mathrm{DFT}} \geq 2(P_{\mathbb{D}^S}+1). \tag{30}$$

Finally, the quantity $E^{i,(p)}_{M,N,P}$ is given in case the incident field is taken to be a uniform plane wave. Then, $\mathbf{E}^i$ follows from

$$\mathbf{E}^i(\boldsymbol{x}) = \mathcal{E}\exp(ik_0\boldsymbol{\theta}\cdot\boldsymbol{x}), \tag{31}$$

in which $\mathcal{E}$ denotes the amplitude of the plane wave and $\boldsymbol{\theta}$ denotes the unit vector of the direction of propagation. The spherical mean (weak form) of this incident field is given by, see [Zwamborn, 1991b],

$$\left[\mathbf{E}^i\right](\boldsymbol{x}) = \mathcal{E}\exp(ik_0\boldsymbol{\theta}\cdot\boldsymbol{x})\frac{12}{(k_0\Delta x)^2}\left[\frac{\sinh(\frac{1}{2}ik_0\Delta x)}{\frac{1}{2}ik_0\Delta x}-\cosh(\tfrac{1}{2}ik_0\Delta x)\right]. \tag{32}$$

The latter weak form is used in the representations for the quantity $E^{i,(p)}_{M,N,P}$ as

$$E^{i,(p)}_{M,N,P} = \left[E^i_p\right](\boldsymbol{x}_{M,N,P} - \tfrac{1}{2}\Delta x_p \boldsymbol{i}_p). \tag{33}$$

Note that, for the limiting case $\Delta x \to 0$, the strong form of the incident uniform plane wave is obtained (cf. Eq. (31)).

Collecting all the results, the weak form of the domain-integral equation is given by Eqs. (10) - (20), (24) and (33). This domain integral equation is symbolically written as

$$e^i = Ld. \tag{34}$$

The latter operator equation is solved numerically by applying a conjugate-gradient iterative scheme, where the DFT's are computed efficiently using fast Fourier transform (FFT) algorithms.

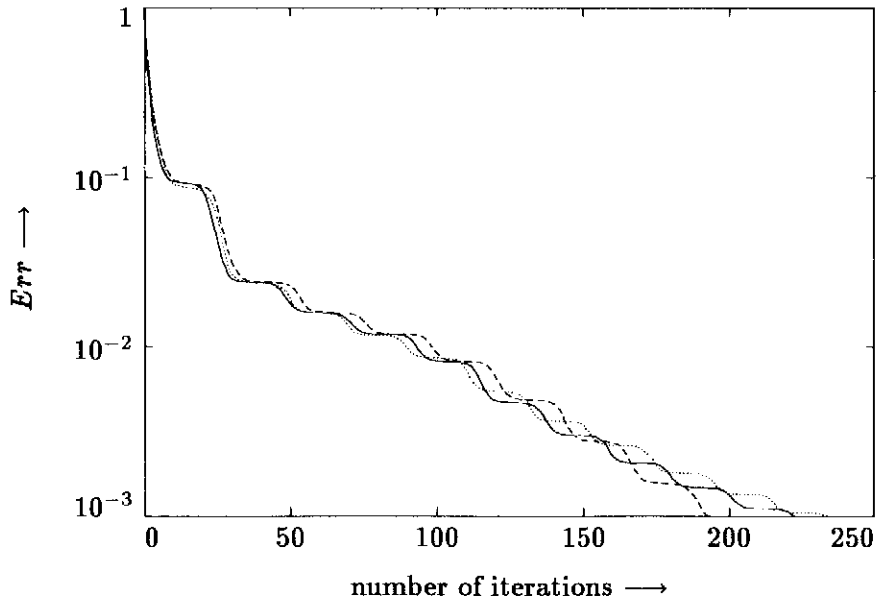

Figure 1: The numerical convergence obtained for the scattering by a inhomogeneous sphere. The numerical results pertaining to a mesh size of $15 \times 15 \times 15$ and $29 \times 29 \times 29$ (Fig. 2) are presented by the dotted line and the solid line, respectively, while the results for the refined mesh (Fig. 3) are presented by the dashed line.

4. Numerical results

The numerical convergence is measured by the normalized root-mean-square error Err

$$Err = \frac{||\mathbf{r}^{(n)}||}{||\mathbf{r}^{(0)}||}, \tag{35}$$

in which $||\mathbf{r}^{(n)}||$ denotes the norm of the residual error in the satisfaction of the operator equation of Eq. (34) over the domain $\mathbb{D}^S$ of the object in the n^{th} iteration. In all cases we have taken a zero initial estimate. All computations were carried out on a VAX 3100/76 workstation in double precision arithmetic. The DFT's are efficiently computed using fast Fourier transform (FFT) algorithms in single precision arithmetic only. The incident field is taken to be a uniform plane wave with (cf. Eq. (32))

$$\mathcal{E}_1 = 1 \text{ V/m}, \quad \mathcal{E}_2 = 0, \quad \mathcal{E}_3 = 0, \tag{36}$$

$$\theta_1 = 0, \quad \theta_2 = 0, \quad \theta_3 = -1, \tag{37}$$

while the frequency of operation is 100 MHz.

We firstly consider a radially layered lossy dielectric spherical object to be present with its origin at $\boldsymbol{x} = \{a, a, a\}$, where a denotes the outer radius of the sphere. It is noted that for this special test case, analytical results are obtained with the Mie series [Kong, 1986]. The relative permittivities

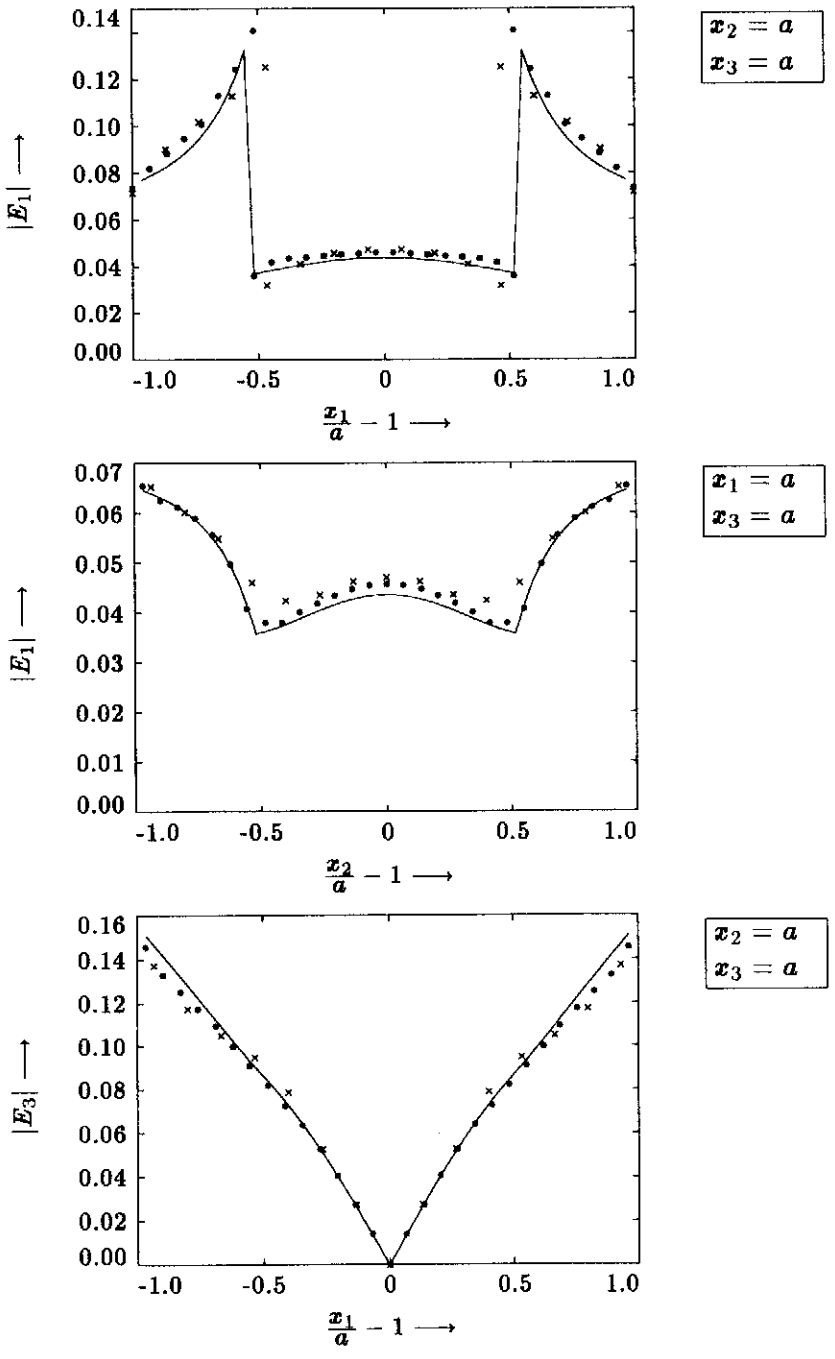

Figure 2: The magnitude of the components of the total electric field inside a lossy inhomogeneous sphere. The numerical results pertaining to a mesh size of $15 \times 15 \times 15$ are presented by the symbols $\times$ and the numerical results pertaining to a mesh size of $29 \times 29 \times 29$ are presented by the symbols $*$. The analytical solution of the inhomogeneous sphere is presented by the solid line.

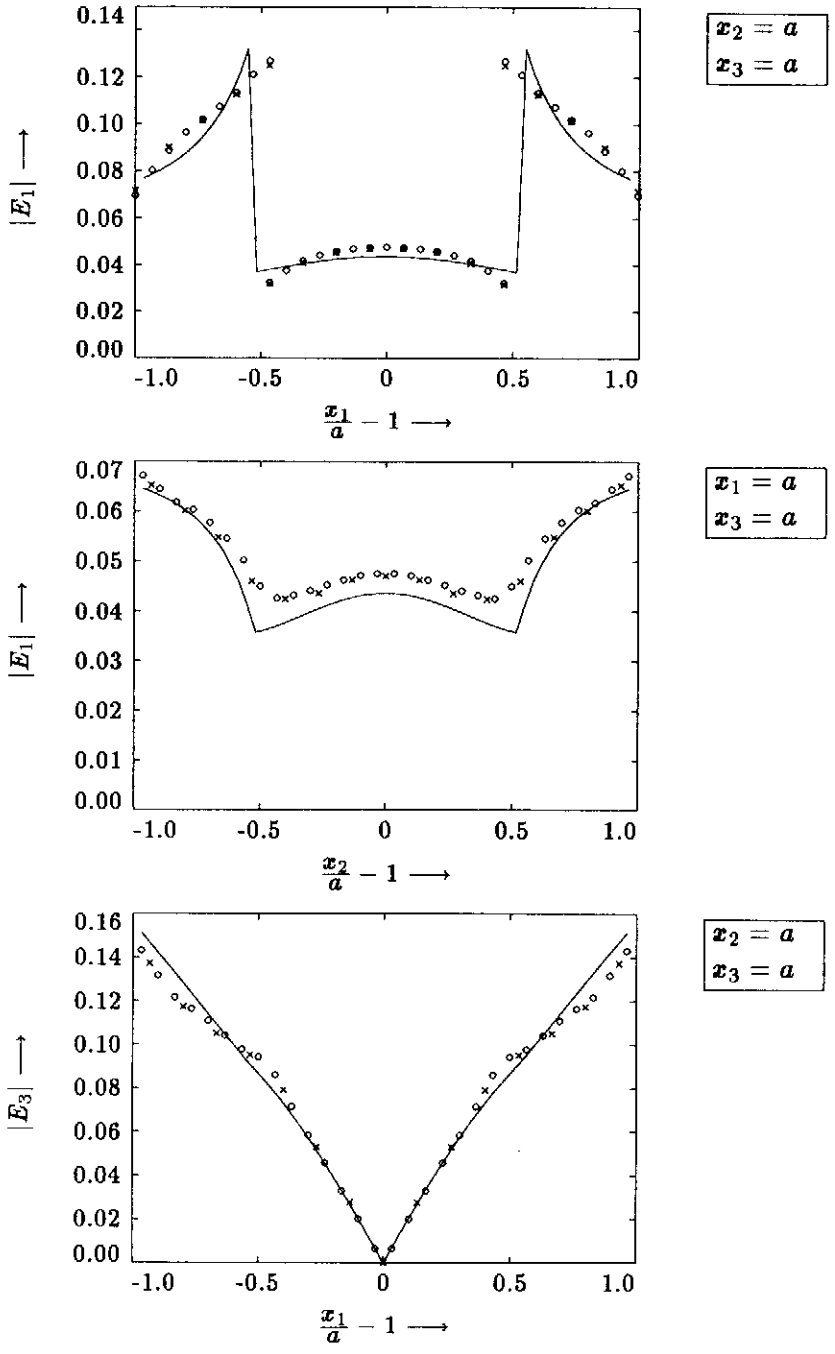

Figure 3: The magnitude of the components of the total electric field inside a $15 \times 15 \times 15$ discretized lossy inhomogeneous sphere. The numerical results pertaining to a mesh size of $15 \times 15 \times 15$ are presented by the symbols $\times$. The discretized object is refined with a mesh size of $30 \times 30 \times 30$ and the numerical results are presented by the symbols $\circ$. The analytical solution of the inhomogeneous sphere is presented by the solid line.

and conductivities are $\varepsilon_{r;1} = 71.5$, $\sigma_1 = 0.83$ S/m, and $\varepsilon_{r;2} = 15$, $\sigma_2 = 0.22$ S/m, respectively. The dimensions are given by $k_0 a_1 = 0.163$ and $k_0 a_2 = 0.314$. It is noted that a_1 denotes the radius of the inner sphere and $a_2 = a$ denotes the radius of the outer sphere. The computations are performed for different mesh sizes of $M_{\mathbf{D}^S} = N_{\mathbf{D}^S} = P_{\mathbf{D}^S} = 15$ ($M_{\mathrm{DFT}} = N_{\mathrm{DFT}} = P_{\mathrm{DFT}} = 32$) and $M_{\mathbf{D}^S} = N_{\mathbf{D}^S} = P_{\mathbf{D}^S} = 29$ ($M_{\mathrm{DFT}} = N_{\mathrm{DFT}} = P_{\mathrm{DFT}} = 64$), respectively. The numerical convergence rate of the iterative scheme is presented in Fig. 1, while the magnitudes of the components of the total electric field are presented in Fig. 2. In order to investigate the discrepancies of the numerical results and the analytical results, we have taken the discretized sphere of the case $M_{\mathbf{D}^S} = N_{\mathbf{D}^S} = P_{\mathbf{D}^S} = 15$ as new object. As next step, this new object has been subdivided with $M_{\mathbf{D}^S} = N_{\mathbf{D}^S} = P_{\mathbf{D}^S} = 30$. The number of iterations to obtain an error less than 0.1 percent is 194. From Fig. 3 it is observed that refining the mesh in the interior of the object yields hardly no improvement. The same discrepancies between the numerical results and the analytical results are observed. The latter reveals that the differences between the analytical and numerical results are caused by the block approximation of the spherical boundary. In order to obtain a better approximation of the spherical boundaries, the discretization of the sphere has to be improved.

As second test case we consider the absorbed power density in a CAT-scan generated model of a human body. In order to arrive at a standard discretized three-dimensional model of a human body, an X-ray computer tomographic scan of one of the present authors, Jaap Mooibroek, has been carried out. A model of $128 \times 128 \times 512$ subdomains with a mesh width of 4 mm in each direction is the result. This so-called "Jaap phantom" consists of muscle with permittivity $\varepsilon_r = 71.5$ and conductivity $\sigma = 0.83$ S/m and fat with permittivity $\varepsilon_r = 15$ and conductivity $\sigma = 0.22$ S/m. In this Jaap phantom we have increased the mesh size with a factor of $4 \times 4 \times 8$ and determined the smallest rectangular domain containing this Jaap phantom. This leads to the reduced Jaap phantom, subdivided with $M_{\mathbf{D}^S} = 21, N_{\mathbf{D}^S} = 31$ and $P_{\mathbf{D}^S} = 53$ and mesh sizes $\Delta x_1 = 1.33751$ cm , $\Delta x_2 = 1.6041$ cm and $\Delta x_3 = 3.1479$ cm . In order to obtain a global impression of the discretized model at hand, we present in Fig. 4 the projection of the Jaap phantom on the (x_1, x_3)-plane and (x_2, x_3)-plane, respectively. The incident field, see Eqs. (32)), (36) and (37), is a plane wave propagating from head to feet. The number of iterations to obtain an error less than 1 percent amounts to 601 iterations. In Figs. 5 - 7, we present the absorbed power density,

$$\dot{w}_h = \tfrac{1}{2}\sigma |\mathbf{E}|^2, \tag{38}$$

together with the tissue composition of the Jaap phantom in some cross-sections. Note that we do not use the Specific Absorption Rate (SAR), since using SAR we also need the values of the volume density of mass. The latter quantity is not significant for solving the electromagnetic field problem. The absorbed power density is normalized to its maximum value in the Jaap phantom. From the latter figures, it is observed that the maximum absorbed power density can be found at the area above the lung. Although the incident plane wave travels from the head to the feet, the absorbed power density has a much smaller value in the area around the brains. This enforces the necessity of having a adequate computer code for the prediction of the electromagnetic field distribution in a strongly inhomogeneous body.

The numerical convergence of the iterative scheme is presented in Fig. 8. In Table 1, the computation time needed to evaluate one iteration on the VAX 3100/76 workstation and the number of unknowns in the the pertaining field problems have been presented. It is noted that the VAX Fortran computer code pertaining to these values is, however, not optimized. Examining this table reveals that the computation time of each iteration is proportional to $(M_{\mathrm{DFT}} \times N_{\mathrm{DFT}} \times P_{\mathrm{DFT}}) [1 + {}^2\log(M_{\mathrm{DFT}} \times N_{\mathrm{DFT}} \times P_{\mathrm{DFT}})]$.

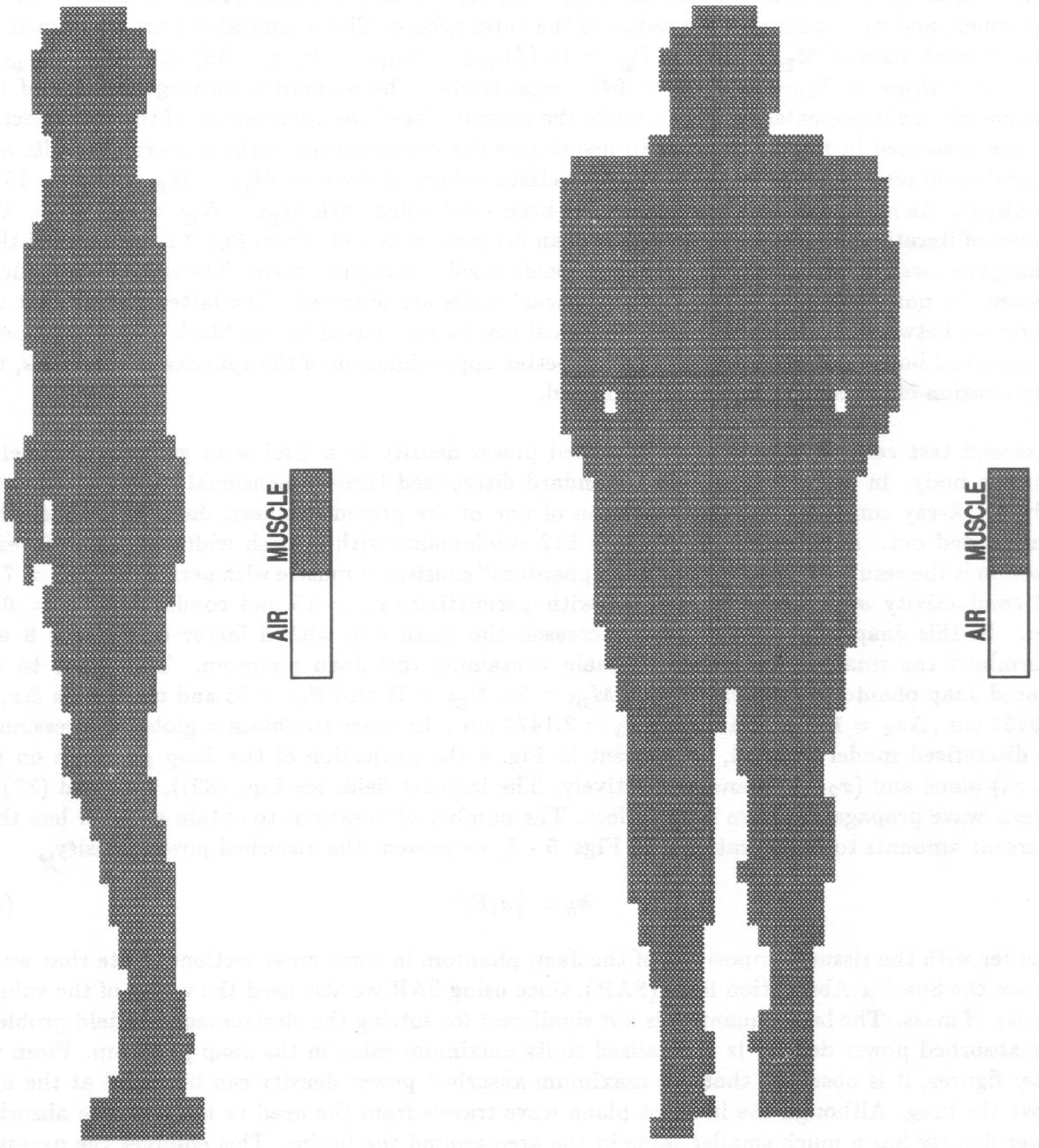

Figure 4: The projection of the Jaap phantom on the plane $x_2 = 0$ (left) and the plane $x_1 = 0$ (right).

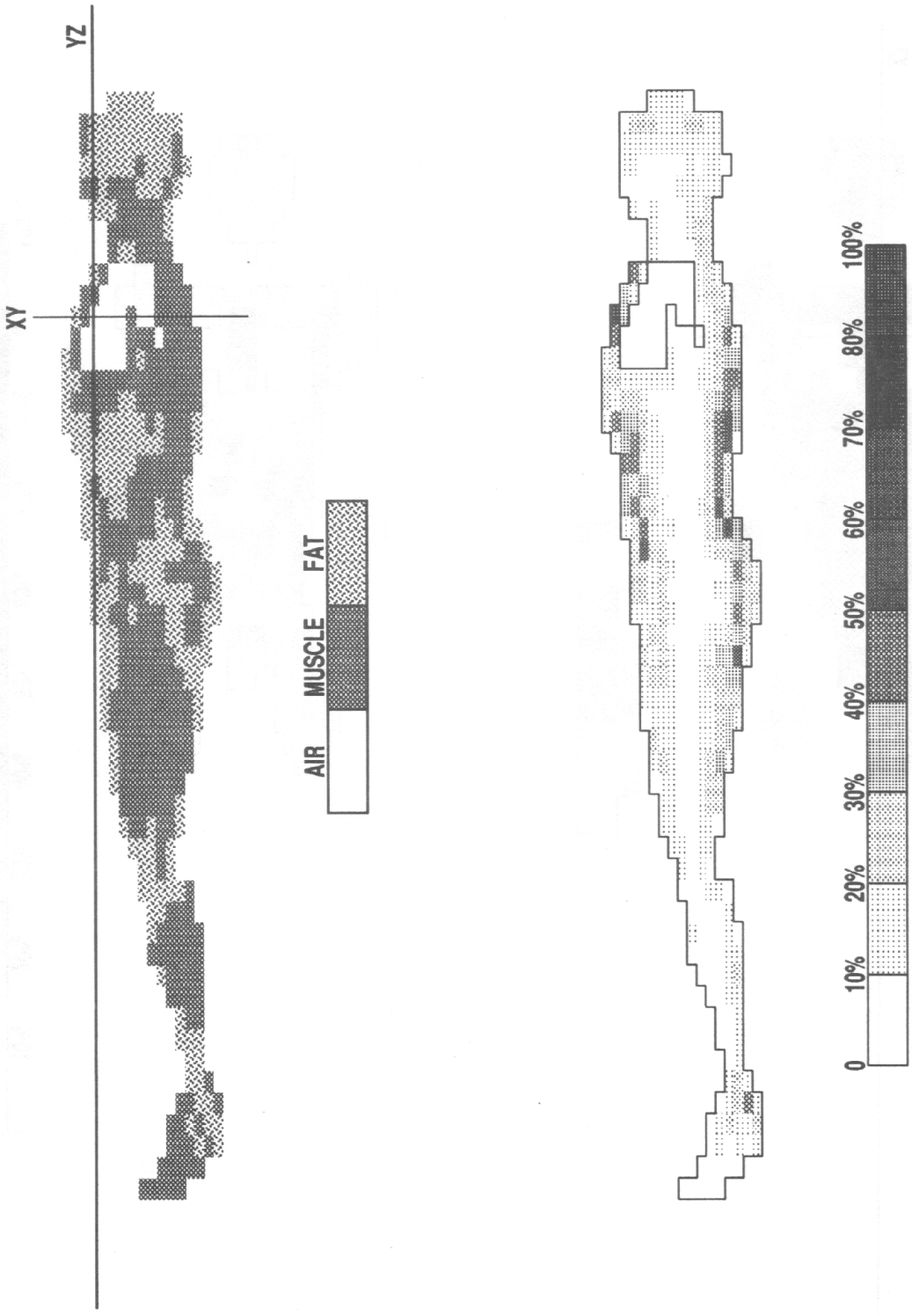

Figure 5: A cross-section of the Jaap phantom (left) and the absorbed power distribution (right) in a sagittal plane XZ.

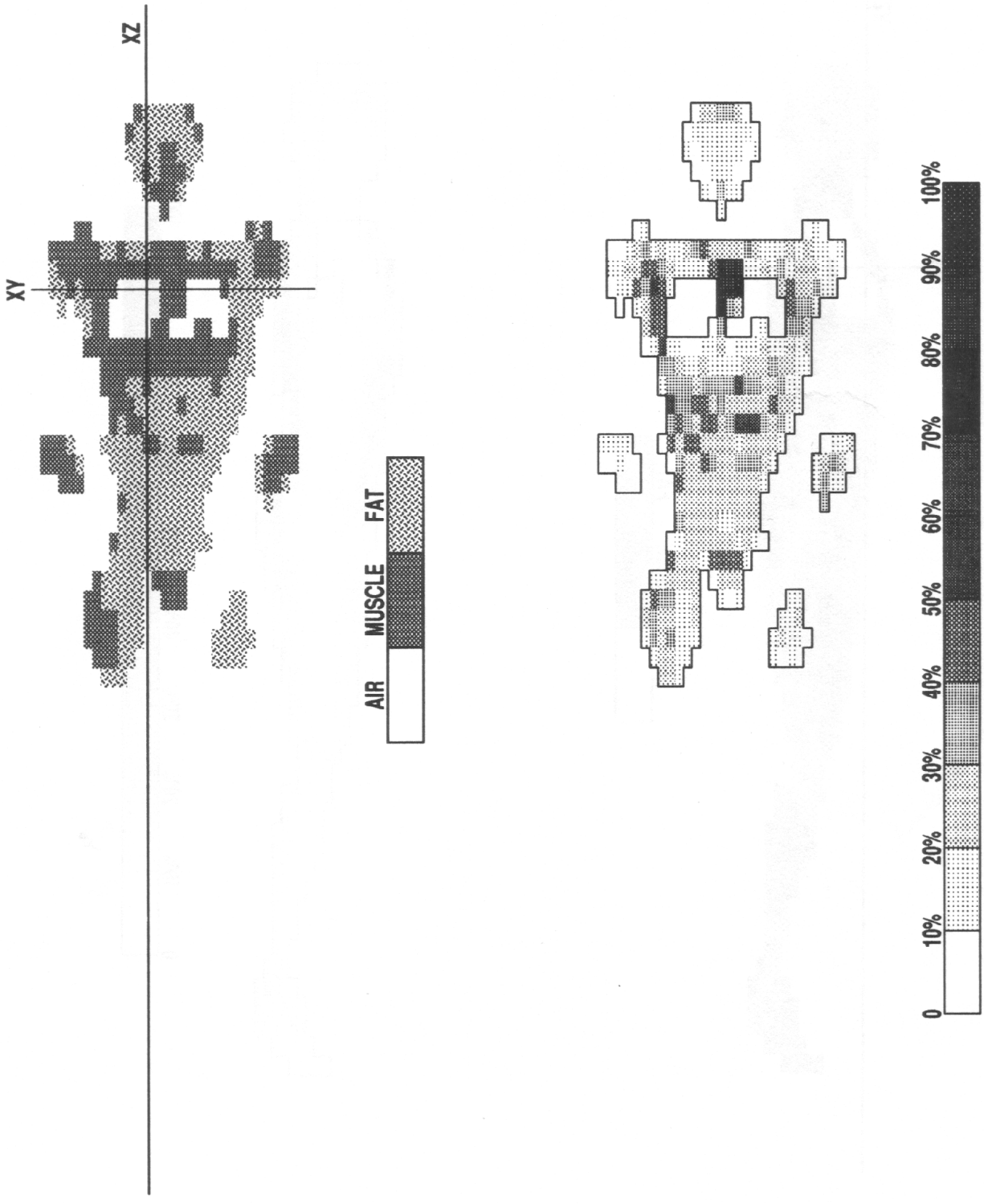

Figure 6: A cross-section of the Jaap phantom (left) and the absorbed power distribution (right) in a coronal plane YZ.

Figure 7: A cross-section of the Jaap phantom (top) and the absorbed power distribution (bottom) in a transverse plane XY.

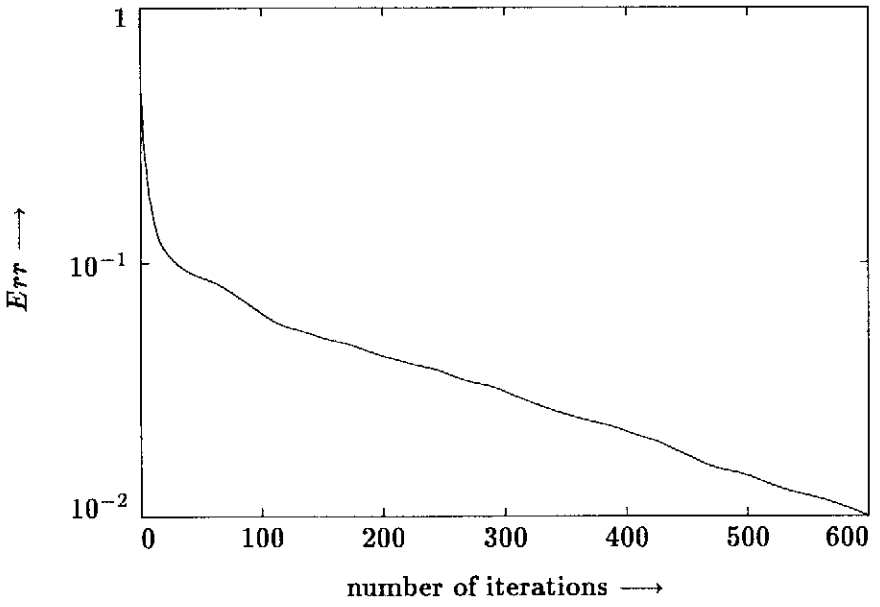

Figure 8: The numerical convergence obtained for the CAT-scan generated model of the human body, the Jaap phantom.

Table 1: Computation time and storage of VAX 3100/76 workstation.

$M_{\mathbf{D}^S} \times N_{\mathbf{D}^S} \times P_{\mathbf{D}^S}$	$M_{\mathrm{DFT}} \times N_{\mathrm{DFT}} \times P_{\mathrm{DFT}}$	number of unknowns	CPU-time of one iteration	computer storage
$15 \times 15 \times 15$	$32 \times 32 \times 32$ (sphere)	10800	0.55 min	5 Mb
$31 \times 31 \times 31$	$64 \times 64 \times 64$ (sphere)	92256	5 min	18 Mb
$21 \times 31 \times 53$	$64 \times 64 \times 128$ (Jaap phantom)	106916	9 min	25 Mb

5. Conclusions

In this paper we have presented a three-dimensional weak formulation of the conjugate-gradient FFT method for strongly inhomogeneous bodies. It is observed that the present weak formulation yields excellent agreement with the analytical results for the radially layered lossy dielectric sphere. Modeling the curved boundaries using a cubical mesh seems to be feasible and the discretization errors tend to vanish for increasingly finer discretizations.

Since we have maintained the simple scalar convolution structure of the vector potential, the computation time of our present weak form is even less than the computation time of the standard conjugate-gradient FFT methods discussed in the Introduction. A realistic model of the human body can now be handled by workstations, the exclusive need of a supercomputer for three-dimensional modeling is not necessary. It is noted that in contrast with the weak formulation of the two-dimensional TE scattering problems presented in [Zwamborn and Van den Berg, 1991a], the present formulation allows the use of different mesh sizes in each Cartesian coordinate. The latter enhances the applicability of the weak formulation to complex, strongly inhomogeneous structures. Finally, it is mentioned that the extension of the present formulation to anisotropic objects is rather straightforward [Zwamborn, 1991b].

6. Acknowledgement

This work was supported under NSF Grant No. DMS-8912593 and a Research Grant from Schlumberger-Doll Research, Ridgefield, CT, U.S.A.

References

N.N. Bojarski [1982], "K-space formulation of the scattering problem in the time domain," *J. Acoust. Soc. Am.*, 72, 570-584.

D.T. Borup, D.M. Sullivan and OM P. Gandi [1987], "Comparison of the FFT conjugate gradient method and the finite-difference time-domain method for the 2-d absorption problem," *IEEE Trans. Microwave Theory Tech.*, MTT-35, 383-395.

M.F. Catedra, E. Gago and L. Nuno [1989], "A numerical scheme to obtain the RCS of three-dimensional bodies of resonant size using the conjugate gradient method and the fast Fourier transform," *IEEE Trans. Antennas Propagat.*, AP-37, 528-537.

M.J. Hagmann [1985], "Comments on 'Limitations of the cubical block model of man in calculating SAR distributions'," *IEEE Trans. Microwave Theory Tech.*, MTT-33, 347-350.

N. Joachimowicz and C. Pichot [1990], "Comparison of three formulations for the 2-D TE scattering problem," *IEEE Trans. Microwave Theory Tech.*, MTT-38, 178-185.

J.A. Kong [1986], "*Electromagnetic wave theory*," John Wiley and Sons, New York.

H. Massoudi, C.H. Durney and M.F. Iskander [1984], "Limitations of the cubical block model of man in calculating SAR distributions," *IEEE Trans. Microwave Theory Tech.*, MTT-32, 746-752.

J.H. Richmond [1965], "Scattering by a dielectric cylinder of arbitrary cross section," *IEEE Trans. Antennas Propagat.*, AP-13, 334-341.

J.H. Richmond [1966], "TE wave scattering by a dielectric cylinder of arbitrary cross-section shape, "*IEEE Trans. Antennas Propagat.,* AP-14, 460-464.

P.M. van den Berg [1984], "Iterative computational techniques in scattering based upon the integrated square error criterion," *IEEE Trans. Antennas Propagat.,* AP-32, 1063-1071.

A.P.M. Zwamborn and P.M. van den Berg [1991], "The weak form of the conjugate gradient method for 2-D TE scattering problems," *IEEE Trans. Microwave Theory Tech.,* MTT-39, 953-960.

A.P.M. Zwamborn [1991], "*Scattering by objects with electric contrast,*" Ph.D.-dissertation, Delft University Press, ISBN 90-6275-691-3/CIP.

A.P.M. Zwamborn and P.M. van den Berg [1992], "The three-dimensional weak form of the Conjugate Gradient FFT method for solving scattering problems," scheduled for publication in the September 1992 issue of *IEEE Trans. Microwave Theory Tech.*